compares closely with the values of 2.412 (2) and 2.419 (2) Å in $MoO_2(L\text{-}NS_2)$.[31] We conclude that nitrate reductase activity by atom transfer is a feasible enzymic reaction pathway. Direct oxo transfer has now been proven to occur, by oxygen labeling studies, in the mechanism of action of xanthine oxidase.[46] Similarly, oxo transfer to and from the catalytic site of *Nitrobacter agilis* nitrite dehydrogenase is required by the results of oxygen and nitrogen isotope labeling.[47] However, it has not been established whether this is a molybdoenzyme.

Lastly, it is noted that Williams[48] in 1973 perceived the possibility of nitrate reduction by atom transfer. Wentworth[49] in 1976 explicitly recognized the minimal reaction $Mo^{IV}O + NO_3^- = Mo^{VI}O_2 + NO_2^-$ as a possible enzymic process. Subsequently, this reaction has been incorporated into mechanistic proposals for nitrate reductase.[6,44] The present work contributes the only well-documented atom transfer reaction of this type in a model system. It, together with our earlier results in analogue reaction systems[15-19] and the isotope labeling study of xanthine oxidase,[46] constitutes a growing base of support for the proposition that many (if not all) reactions of the molybdenum hydroxylases involve one step of atom transfer.[14]

Acknowledgment. This research was supported by National Science Foundation Grant CHE 85-21365. We thank E. W. Harlan for useful discussions and Professor K. V. Rajagopalan for a preprint of ref 11b.

(46) Hille, R.; Sprecher, H. *J. Biol. Chem.* **1987**, *262*, 10914.
(47) Friedman, S. H.; Massefski, W., Jr.; Hollocher, T. C. *J. Biol. Chem.* **1986**, *261*, 10538.
(48) Williams, R. J. P. *Biochem. Soc. Trans.* **1973**, *1*, 1. See also: Steifel, E. I. *Proc. Natl. Acad. Sci. U.S.A.* **1973**, *70*, 988.
(49) Wentworth, R. A. D. *Coord. Chem. Rev.* **1976**, *18*, 1.

Gold-Rhodium and Gold-Iridium Hydride Clusters

Alberto Albinati,[1a] Francesco Demartin,[1a] Philipp Janser,[1b] Larry F. Rhodes,[1b] and Luigi M. Venanzi*[,1b]

Contribution from the Laboratorium für Anorganische Chemie, ETH-Z, CH-8092 Zürich, Switzerland, and Istituto di Chimica Farmaceutica, Università di Milano, I-20131 Milano, Italy.
Received June 24, 1988

Abstract: The hydrides $MH_3(tripod)$ (M = Rh and Ir; tripod = triphos and triars) react with $[Au(L)]^+$ cations to give heterometallic species of the types $[(tripod)MH_3Au(L)]^+$, type **A**, $[(tripod)MH_3\{Au(L)\}_2]^{2+}$, type **B**, and $[(tripod)MH_2\{Au(L)\}_3]^{2+}$, type **C**. The complexes of type **A** can be described as containing one M-H-Au unit which, however, is still dynamic at -90 °C. Similar behavior is observed for the complexes of type **B** where two M-H-Au units are present. The complexes of type **C** contain only two hydride ligands. The X-ray crystal structure of $[(triphos)RhH_2\{Au(PPh_3)\}_3](CF_3SO_3)_2$ shows the presence of a $RhAu_3$ tetrahedron with the rhodium capped by triphos, while each gold atom is coordinated to one PPh_3. The hydride ligands could not be located, but it is proposed that they may occupy two $RhAu_2$ triangular faces. Crystal data: space group $R3c$, a = 20.343 (3) Å, c = 44.937 (7) Å, Z = 6, V = 16104.9 Å^3, ρ(calcd) = 1.486 g cm^{-3}, and R = 0.049.

Interest in transition-metal clusters has centered around the use of these species as models for heterogeneous catalysts.[2] Recent studies have also shown how unusually large clusters begin to mimic the properties of bulk metals.[3] Obviously, this is an area in which the rational synthesis of clusters would be beneficial. The stoichiometric incorporation of certain metal fragments in clusters would not only change the size of the clusters but may influence the subsequent physical and chemical properties of the cluster.

A significant role in the synthesis of gold and gold heterometallic clusters has been played by the fragment, $[Au(L)]^+$ (L = phosphine or other two-electron donors). Gold clusters can be made by $NaBH_4$ reduction of $[Au(L)]^+$ units.[4] Similarly, treatment of transition-metal hydrides by $[Au(L)]^+$ yields gold heterometallic clusters.[5]

Our interest in the synthesis of hydride-bridged heterometallics produced from metal hydrides and unsaturated, electrophilic metal complexes[6] prompted the synthesis and structural characterization of one of the first gold hydrides, $[(PPh_3)_3H_2Ir(\mu\text{-}H)Au(PPh_3)]^+$ (I).[7] Since this initial report, several other bimetallic aggregates resulting from rhodium and iridium trihydrides and group 11 electrophiles have been reported.[8] The fact that $IrH_3(PPh_3)_3$ can be isolated as mer and fac isomers provides the unique opportunity to study cluster formation as a function of geometry. While two group 11 electrophiles are supported on a meridional hydride template,[8d] the facial hydride template can accommodate up to three, all with rather short contacts to one another.[9] Thus, the facial arrangement appears to better facilitate cluster growth.

With this in mind, we have investigated the addition of successive equivalents of gold(I) phosphine and arsine units to the facial trihydrides, $MH_3(tripod)$ (where M = Rh or Ir and tripod = $CH_3C(CH_2EPh_2)_3$, E = P (triphos) or As (triars)). As a result of this study we now report (1) the synthesis and characterization of gold heterometallic clusters containing one, two, and three

(1) (a) Università di Milano. (b) ETH Zürich.
(2) (a) Muetterties, E. L.; Rodin, T. N.; Band, E.; Brucker, C. F.; Pretzer, W. R. *Chem. Rev.* **1979**, *79*, 91. (b) Braunstein, P.; Rose, J. *Stereochemistry of Organometallic and Inorganic Compounds*; Bernal, I., Ed.; Elsevier: Amsterdam 1988; 3, in press. (c) Johnson, B. F. G.; Benfield, R. E. *Transition Metal Clusters*; Johnson, B. F. G., Ed.; Wiley: New York, 1980; pp 471-606.
(3) Teo, B. K.; Keating, K.; Hao, Y. H. *J. Am. Chem. Soc.* **1987**, *109*, 3494 and references quoted therein.
(4) Hall, K. P.; Mingos, D. M. P. *Prog. Inorg. Chem.* **1984**, *32*, 237.
(5) Alexander, B. D.; Johnson, B. J.; Johnson, S. M.; Casalnuovo, A. L.; Pignolet, L. H. *J. Am. Chem. Soc.* **1986**, *108*, 4409 and references quoted therein.
(6) Venanzi, L. M. *Coord. Chem. Rev.* **1982**, *43*, 251.
(7) (a) Lehner, H.; Matt, D.; Pregosin, P. S.; Venanzi, L. M.; Albinati, A. *J. Am. Chem. Soc.* **1982**, *104*, 6825. (b) Green, M.; Orpen, A. G.; Salter, I. D.; Stone, F. G. A. *J. Chem. Soc., Chem. Commun.* **1982**, 813.
(8) (a) Rhodes, L. F.; Huffman, J. C.; Caulton, K. G. *J. Am. Chem. Soc.* **1984**, *106*, 6874. (b) Rhodes, L. F.; Huffman, J. C.; Caulton, K. G. *J. Am. Chem. Soc.* **1985**, *107*, 1759. (c) Bachechi, F.; Ott, J.; Venanzi, L. M. *J. Am. Chem. Soc.* **1985**, *107*, 1760. (d) Braunstein, P.; Carneiro, T. M. G.; Matt, D.; Tiripichio, A.; Camellini, M. *Angew. Chem., Int. Ed. Engl.* **1986**, *25*, 748. (e) Rhodes, L. F. Ph.D. Dissertation, Indiana University, 1984. (f) Ott, J. Ph.D. Dissertation, ETH Nr. 8000, Zürich, 1986.
(9) In ref 7b, the Cu-Cu distance is 2.570 Å, while that found in Cu metal is 2.55 Å. Wells, A. F. *Structural Inorganic Chemistry*; Oxford University Press: London, 1975.

0002-7863/89/1511-2115$01.50/0

Table I. List of Complexes[a]

type A compounds	type B compounds	type C compounds
$[(triphos)RhH_3Au(PPh_3)]^+$, **A1**	$[(triphos)RhH_3\{Au(PPh_3)\}_2]^{2+}$, **B1**	$[(triphos)RhH_2\{Au(PPh_3)\}_3]^{2+}$, **C1**
$[(triphos)IrH_3Au(PPh_3)]^+$, **A4**	$[(triphos)IrH_3\{Au(PPh_3)\}_2]^{2+}$, **B4**	$[(triphos)RhH_2\{Au(AsPh_3)\}_3]^{2+}$, **C2**
$[(triphos)IrH_3Au(PEt_3)]^+$, **A5**	$[(triphos)IrH_3\{Au(PEt_3)\}_2]^{2+}$, **B5**	$[(triars)RhH_2\{Au(AsPh_3)\}_3]^{2+}$, **C3**
$[(triphos)IrH_3Au(P(i\text{-}Pr)_3)]^+$, **A6**	$[(triphos)IrH_3\{Au(P(i\text{-}Pr)_3)\}_2]^{2+}$, **B6**	$[(triphos)IrH_2\{Au(PPh_3)\}_3]^{2+}$, **C4**
$[(triphos)IrH_3Au(P(o\text{-}Tol)_3)]^+$, **A7**	$[(triphos)IrH_3\{Au(P(o\text{-}Tol)_3)\}_2]^{2+}$, **B7**	$[(triphos)IrH_2\{Au(AsPh_3)\}_3]^{2+}$, **C8**
$[(triphos)IrH_3Au(AsPh_3)]^+$, **A8**	$[(triphos)IrH_3\{Au(AsPh_3)\}_2]^{2+}$, **B8**	$[(triars)IrH_2\{Au(PPh_3)\}_3]^{2+}$, **C10**
$[(triphos)IrH_3Au(As(i\text{-}Pr)_3)]^+$, **A9**	$[(triphos)IrH_3\{Au(As(i\text{-}Pr)_3)\}_2]^{2+}$, **B9**	

[a] The letters A, B, and C indicate the number of coordinated gold cations (1, 2, or 3, respectively).

Table II. Relevant ^{31}P NMR and ^1H NMR Data

compd	temp[d]	^{31}P NMR	^1H NMR
A1	RT	+48.1, br multiplet; +29.3, d × d, $^1J(Rh,H)$ = 97, $^4J(P,P)$ = 10 Hz	−5.7, d × d × d, $^2J(P^{tr},H)$ = 112 Hz, $^2J(P^{Au},H)$ = 40 Hz, $^1J(Rh,H)$ = 15 Hz
B1	RT	+44.2, q × d, $^4J(P,P)$ = 16, $^3J(Rh,P^{Au})$ = 13 Hz; +30.8, t × d, $^4J(P,P)$ = 16, $^1J(Rh,P^{tr})$ = 93 Hz	−4.1, complex d × t × d, $^2J(P^{tr},H)$ = 66 Hz, $^2J(P^{Au},H)$ = 25 Hz, $^1J(Rh,H)$ = 14 Hz
C1	RT	+43.9, q × d, $^4J(P,P)$ = 28, $^3J(Rh,P^{Au})$ = 11 Hz; +36.9, q × d, $^4J(P,P)$ = 28, $^1J(Rh,P^{tr})$ = 100 Hz	−4.3, complex q × q × d, $^2J(P^{tr},H)$ = 15 Hz; $^2J(P^{Au},H)$ = 11 Hz; $^1J(Rh,H)$ = 11 Hz
C2	RT	+34.0, d, $^1J(Rh,P)$ = 101 Hz	−5.7, q × d, $^2J(P,H)$ = 27 Hz, $^1J(Rh,H)$ = 12 Hz
C3[c]	RT		−7.5, d, $^1J(Rh,H)$ = 13 Hz
A4	−90 °C	+52.9, q, $^4J(P,P)$ = 15 Hz; −3.0, d, $^4J(P,P)$ = 15 Hz	−8.0, m, $^2J(P^{Au},H)$ = 25 Hz; $\|N\|$[b] = 75 Hz
B4	RT	+49.7, q, $^4J(P,P)$ = 17 Hz; −4.3, t, $^4J(P,P)$ = 17 Hz	−6.3, t × d complex, $^2J(P^{Au},H)$ = 26 Hz, $^2J(P^{tr},H)$ = 47 Hz
C4	RT	+50.6, q, $^4J(P,P)$ = 24 Hz; −1.0, broad singlet	−5.8, m complex
	+80 °C	+50.1, q, $^4J(P,P)$ = 25 Hz; −2.6, q, $^4J(P,P)$ = 25 Hz	−6.0, q × q, $^2J(P^{tr},H)$ = 48 Hz, $^2J(P^{Au},H)$ = 12 Hz
	−40 °C	+50.2, t × d, $^4J(P^{Au},P^b)$ = 15 Hz, $^4J(P^{Au},P^a)$ = 41 Hz; +6.5, t × q, $^2J(P^a,P^b)$ = 19 Hz, $^4J(P^a,P^{Au})$ = 41 Hz; −0.6, d × q, $^2J(P^p,P^a)$ = 19 Hz, $^4J(P^b,P^{Au})$ = 15 Hz	−5.6, d × q, $^2J(P^{tr},H)$ = 16 Hz, $^2J(P^{Au},H)$ = 12 Hz
A5	−80 °C	+53.2, q, $^4J(P,P)$ = 14.5 Hz; −3.0, d, $^4J(P,P)$ = 14.5 Hz	−8.1, br d, $^2J(P^{tr},H)$ = 82 Hz
B5	RT	+51.4, q, $^4J(P,P)$ = 16 Hz; −3.9, t, $^4J(P,P)$ = 16 Hz	−6.4, t × d complex, $^2J(P^{Au},H)$ = 24 Hz, $^2J(P^{tr},H)$ = 50 Hz
A6	−80 °C	+81.3, q, $^4J(P,P)$ = 14 Hz; −2.8, d, $^4J(P,P)$ = 14 Hz	−7.9, m, $^2J(P^{Au},H)$ = 30 Hz, $\|N\|$[b] = 73 Hz
B6	RT	+81.8, q, $^4J(P,P)$ = 15.5 Hz; −5.3, t, $^4J(P,P)$ = 15.5 Hz	−6.3, t × d complex, $^2J(P^{Au},H)$ = 23 Hz, $^2J(P^{tr},H)$ = 50 Hz
A7	RT	+33.1, q, $^4J(P,P)$ = 16 Hz; −4.1, d, $^4J(P,P)$ = 16 Hz	−8.4, m, $^2J(P^{Au},H)$ = 32 Hz, $\|N\|$[b] = 69 Hz
B7	RT	+37.1, q, $^4J(P,P)$ = 17.5 Hz; −7.3, t, $^4J(P,P)$ = 17.5 Hz	−6.8, t × d complex, $^2J(P^{Au},H)$ = 25 Hz, $^2J(P^{tr},H)$ = 48 Hz
A8	RT, −80 °C	−4.3, br s	−8.4, m, $\|N\|$[c] = 72 Hz
B8	RT, −80 °C	−3.8, br s	−6.5, m, $\|N\|$[c] = 48 Hz
C8	RT, −80 °C	−5.5, br s; −3.3, t, $^2J(P^a,P^b)$ = 17 Hz; −11.3, d, $^2J(P^b,P^a)$ = 17 Hz	−7.1, br q, $^2J(P,H)$ = 17 Hz; −6.9, m, $\|N\|$[c] = 53 Hz
A9	RT, −80 °C	−3.3, br s	−8.2, m, $\|N\|$[c] = 72 Hz
B9	RT, −80 °C	−5.0, br s	−6.5, m, $\|N\|$[c] = 49 Hz
C10		+51.7, s	−8.2, q, $^2J(P^{Au},H)$ = 11 Hz

[a] ^{103}Rh NMR: δ = 96 ppm, t, $^1J(Rh,H)$ = 13 Hz. [b] (AA'A''MXX'X'') spin system centered at the chemical shift (ppm) given by the first number. According to the notation by Jones et al. (Jones, R. G.; Hirst, R. C.; Bernstein, H. J. *Can. J. Chem.* **1965**, *43*, 683), $|N|$ means the large separation between the biggest peaks of the AA'A''XX'X'' system and is the sum of $J(A,X) + 2J(A,X')$. [c] (AA'A''XX'X'') spin system centered at the chemical shift (ppm) given by the first number. See also footnote *c*. [d] RT stands for room temperature.

gold(I) fragments per M(tripod) unit; (2) the crystal and molecular structure of $[(triphos)Ru(\mu\text{-}H)_2\{Au(PPh_3)\}_3]^{2+}$; and (3) the effects of the steric and electronic properties of phosphine and arsine ligands coordinated to gold on the growth of these clusters.

Results and Discussion

Three distinct sets of compounds can be formed by treatment of $MH_3(tripod)$ (M = Rh and Ir; tripod = triphos and triars) with different amounts of the cations $[Au(THF)(L)]^+$ (L = tertiary phosphine or arsine) (prepared in situ from the corresponding AuCl(L) species and $Tl[PF_6]$ or $AgCF_3SO_3$ in THF). Their composition differs depending on the M:Au molar ratios, i.e., $[(tripod)MH_3Au(L)]^+$, type **A**, $[(tripod)MH_3\{Au(L)\}_2]^{2+}$, type **B**, and $[(tripod)MH_2\{Au(L)\}_3]^{2+}$, type **C**. The compounds characterized are listed in Table I.

Complexes $[(tripod)MH_3Au(L)]^+$, Type A. These are produced in good yields using a 1:1 ratio of reagents (eq 1).

$$MH_3(tripod) + [Au(THF)(L)]^+ \xrightarrow[THF]{CH_2Cl_2} [(tripod)MH_3Au(L)]^+ \quad (1)$$
type A

M = Rh and Ir; tripod = triphos and triars;
L = tertiary phosphine or arsine

Most informative are the ^{31}P and ^1H NMR data (in the hydride region) (see Table II). These are best illustrated by using the cation **A4** whose static structure can be formulated as shown below.

The ^{31}P NMR spectrum of this compound consists of a doublet assigned to the phosphorus atoms of triphos, P^{tr}, and a broad signal

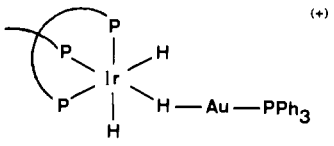

A4

assigned to the phosphorus atom coordinated to gold, P^{Au}. However, at −90 °C the latter signal sharpens to a quartet. As the P^{tr} signals do not show further splitting this complex retains some fluxionality even at this temperature.

The ^{31}P NMR spectra of the other compounds give the patterns expected on the basis of their NMR active nuclei. Exceptions are $[(triphos)RhH_3Au(PPh_3)]^+$, **A1**, whose P^{Au} signal does not sharpen even at −80 °C and $[(triphos)IrH_3Au(P(o\text{-}Tol)_3)]^+$, **A7**, which gives sharp signals at room temperature.

The room temperature ^1H NMR spectra of complexes of type **A** are of higher order as found for the parent compounds $MH_3(triphos)$[10,11] and consist of two broad signals which, at lower temperature, show indications of multiplicity.

An exception to this is provided by $[(triphos)IrH_3Au(P(o\text{-}Tol)_3)]^+$, **A7**. Its room temperature spectrum, shown in Figure 1b, corresponds to that of $IrH_3(triphos)$ (see Figure 1a) doubled up. This doubling disappears on selective decoupling at the P^{Au} frequency (see Figure 1c), while decoupling of the P^{tr} atoms leaves the doublet shown in Figure 1d. As for in closely related cases, e.g., $[(triphos)IrH_3(HgR)]^+$,[12] the H resonance shifts downfield as it becomes coordinated to the second metal atom.

As expected, the observed multiplicities depend on the nature of the metal and the uncharged ligands. In the case of $[(triphos)RhH_3Au(PPh_3)]^+$, **A1**, the value of $^1J(^{103}Rh,^1H)$ is 15 Hz as compared with 20 Hz in $RhH_3(triphos)$.[10]

The IR spectra of compounds of this type show bands which can be associated with the presence of both terminal and bridging ligands. The spectrum of $[(triphos)IrH_3Au(P(i\text{-}Pr)_3)]^+$, **A6**, is shown in Figure 2a. However, given the expected low molecular symmetry of the compounds band assignments were not attempted.

The static structure proposed for complexes of type **A** is based on the X-ray crystal structure of $[(PPh_3)_3H_2Ir(\mu\text{-}H)Au(PPh_3)]^+$ (I),[7a] $[(CO)_5Cr(\mu\text{-}H)Au(PPh_3)]^+$ (II),[7b] and $[(C_6F_5)(PEt_3)_2Pt(\mu\text{-}H)Au(PPh_3)]^+$ (III).[13] In each case the metal–gold vector is bridged by a single hydride. It should be noticed that in all cases the M, Au, and P atoms are not linear.

Evans and Mingos have shown that, in mononuclear gold phosphine fragments, the d orbitals are essentially part of the core leaving the empty (for Au cations) hy(s-z) hybrid orbital and a p_x,p_y degenerate pair available for bonding.[14] However, the large d–p promotion energy[15] results in the p_x,p_y orbitals residing too high in energy to contribute significantly to bonding. Therefore, the hy(s–z) hybrid orbital is the primary bonding orbital in gold(I) phosphines.

These considerations suggest that the primary interaction between a transition-metal hydride and a gold(I) phosphine fragment is the donation of the two electrons contained in the metal–hydride bond into the empty gold(I) hy(s–z) hybrid orbital. This is presumably what occurs in compounds II and III.[7b,13] However, the rather short metal–gold bond distances (2.714 (1) and 2.770 (2) Å) found in these two complexes are suggestive of significant metal-gold bonding. This, and the fact that the metal–hydride–gold angles in II and III are rather acute (111° and 103°, respectively), can be interpreted as representative of a closed, 3-center, 2-electron interaction[16] or as indicative of significant interaction of an empty gold p orbital and a filled component of the "t_{2g}" remnants of the heteroatom.[13] With regard to the latter interpretation, the transition metals in complexes I, II, and III are electron-rich and contain filled pseudo t_{2g} orbitals.

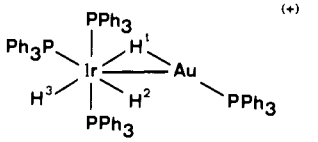

I

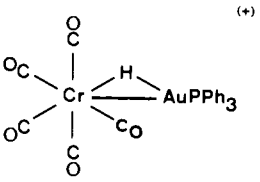

II

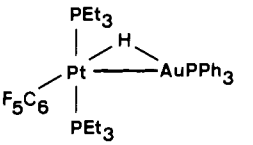

III

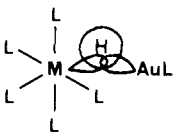

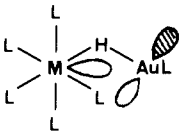

It has been pointed out elsewhere[17] that the L–M–H unit (M = Ag(I) or Au(I)) is isolobal with H_2; and, therefore, complexes of type **A** might also be represented as shown schematically below.

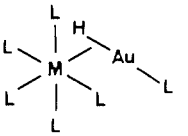

The bonding scheme for I (and for complexes of type **A**) is complicated by the presence of *cis*-dihydride unit. In this case, significant donation of electron density from the second metal–hydride moiety to the gold could occur as does in $[(dppm)_2Ru(\mu\text{-}H)_2Au(PPh_3)]^+$ (IV) (dppm = $Ph_2PCH_2PPh_2$).[18] Bonding

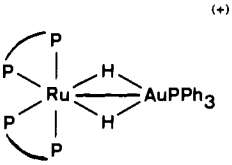

IV

interactions of this type may be responsible for rather facile fluxionality of $[AuL]^+$ found in I (static structure observed at −40 °C[19]) and type **A** complexes (see above). The correct bonding picture for the type **A** complexes awaits an X-ray structural determination.

While $J(P^{Au},\mu\text{-}H)$ is rather large (ranging from 79 to 105 Hz in I, II, III), the analogous couplings for compounds **A1**, **A4**, **A5**,

(10) Ott, J.; Venanzi, L. M.; Ghilardi, C. A.; Midollini, S.; Orlandini, A. *J. Organomet. Chem.* **1985**, *291*, 89 and references quoted therein.
(11) Janser, P.; Venanzi, L. M.; Bachechi, F. *J. Organomet. Chem.* **1985**, *296*, 229 and references quoted therein.
(12) McGilligan, B. S.; Venanzi, L. M.; Wolfer, M. *Organometallics* **1987**, *6*, 946.
(13) Albinati, A.; Lehner, H.; Venanzi, L. M.; Wolfer, M. *Inorg. Chem.* **1987**, *26*, 3933.
(14) Evans, D. G.; Mingos, D. M. P. *J. Organomet. Chem.* **1982**, *232*, 171.
(15) Mingos, D. M. P. *Chem. Soc. Rev.* **1986**, *15*, 31.
(16) Olsen, J. P.; Koetzle, T. F.; Kirtley, S. W.; Andrews, M.; Tipton, D. L.; Bau, R. *J. Am. Chem. Soc.* **1974**, *96*, 6621.
(17) Albinati, A.; Demartin, F.; Venanzi, L. M.; Wolfer, M. *Angew. Chem., Int. Ed. Engl.* **1988**, *27*, 563.
(18) Alexander, B. D.; Johnson, B. J.; Johnson, S. M.; Boyle, P. D.; Kann, N. C.; Mueting, A. M.; Pignolet, L. H. *Inorg. Chem.* **1987**, *26*, 3506.
(19) Lehner, H. Ph.D. Dissertation, ETH Nr. 7239, Zürich, 1983.

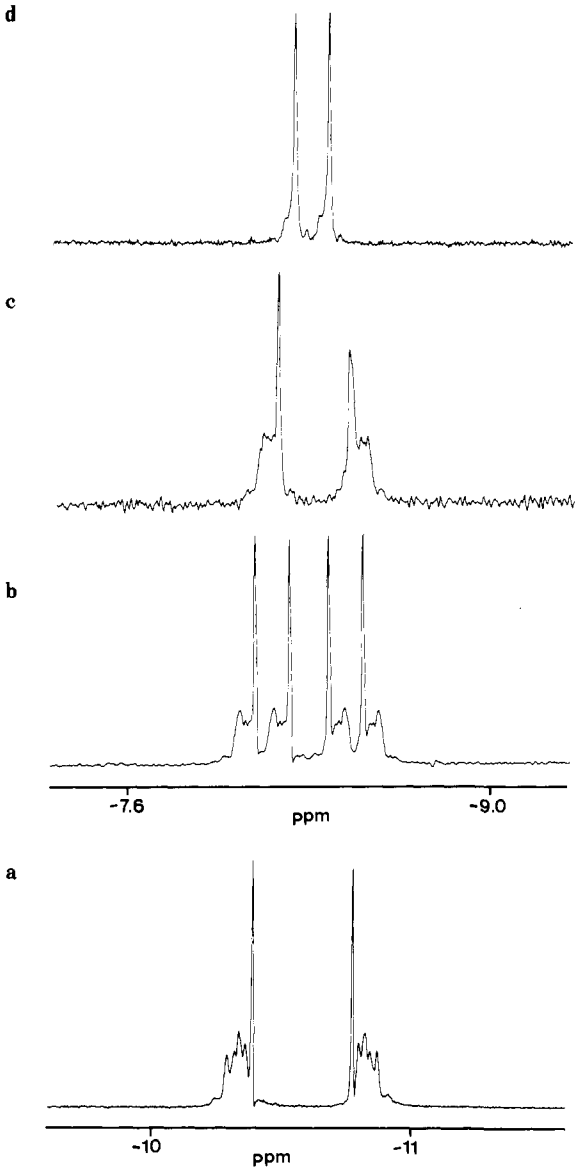

Figure 1. (a) 250 MHz ^1H NMR spectrum of IrH_3(triphos); (b) 250 MHz ^1H NMR spectrum of [(triphos)$IrH_3Au(P(o\text{-}Tol)_3)$][$(CF_3SO_3)$], [A7]$(CF_3SO_3)$; (c) 250 MHz $^1H\{^{31}P\}$ NMR spectrum of [A7](CF_3SO_3), decoupled at the ^{31}P resonance of P^{Au}; (d) 250 MHz $^1H\{^{31}P\}$ NMR spectrum of [A7](CF_3SO_3), decoupled at the ^{31}P resonance of P^{tr}.

and **A6** vary from 25 to 40 Hz. This smaller coupling is entirely consistent with a highly fluxional gold phosphine fragment in the type **A** complexes (even at −80 °C), inasmuch as the coupling is now averaged over three equivalent hydride sites.[20] Similar averaging of coupling constants due to dynamic behavior has been previously observed in complexes $[(triphos)IrH_3(HgR)]^+$.[12] However, the possibility of the decreased coupling arising from a rapid equilibrium between trans and cis P–Au–(μ-H) linkages cannot be excluded.[18]

Complexes [(tripod)MH_3{Au(L)}$_2]^{2+}$, Type B. When the complexes MH_3(tripod) and $[Au(THF)(L)]^+$ are reacted in a 1:2 ratio, complex cations of type **B** are obtained (eq 2).

$$MH_3(tripod) + 2[Au(THF)(L)]^+ \xrightarrow[THF]{CH_2Cl_2} [(tripod)MH_3\{Au(L)\}_2]^{2+} \quad (2)$$
type **B**

M = Rh and Ir; tripod = triphos and triars;
L = tertiary phosphine or arsine

(20) The energy barrier to intramolecular exchange in gold phosphine clusters is low (see ref 4).

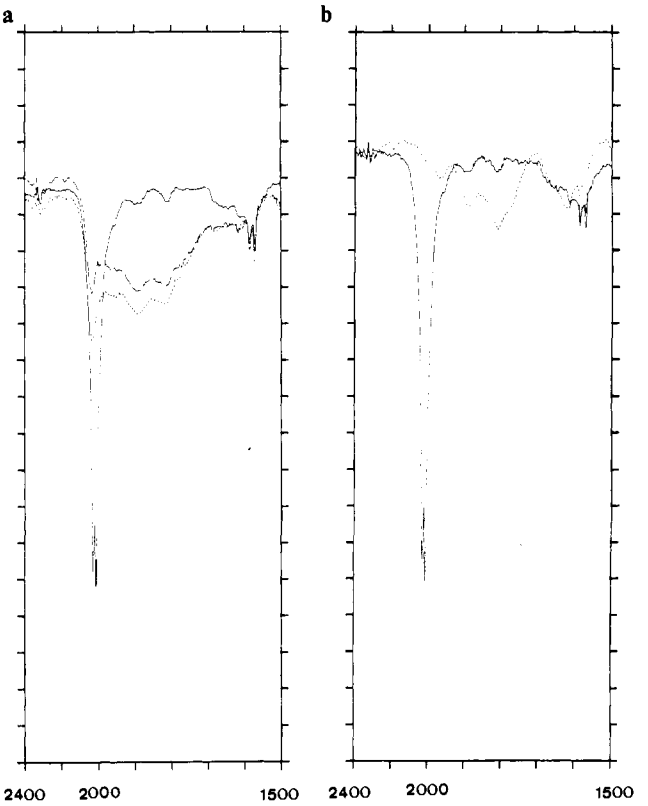

Figure 2. (a) IR spectra of IrH_3(triphos)(—), [(triphos)$IrH_3Au(P(i\text{-}Pr)_3)$][$(CF_3SO_3)$], [A6]$(CF_3SO_3)$(···), and [(triphos)$IrH_3${$Au(P(i\text{-}Pr)_3)$}$_2$][$(CF_3SO_3)_2$, [B6]$(CF_3SO_3)_2$ (−−); (b) IR spectra of IrH_3(triphos) (—) and [(triphos)IrH_2{$Au(PPh_3)$}$_3$][$(CF_3SO_3)_2$, [C4]$(CF_3SO_3)_2$(···).

Also for the compounds of this type ^{31}P and ^1H NMR spectra (in the hydride regions) prove particularly informative (see Table II). These will be illustrated by using compound **B4** formulated schematically as shown below.

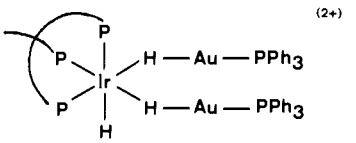

B4

The room temperature ^{31}P NMR spectrum shows a triplet assigned to the P^{tr} atoms and a quartet assigned to the P^{Au} atoms. The ^{31}P NMR spectra of the other compounds show the multiplicity changes expected when iridium is replaced by rhodium and phosphorus by arsenic. These spectra show no significant temperature dependence down to −90 °C.

The room temperature ^1H NMR spectra of compounds of this type are complex and are best illustrated by considering Figure 3 which shows the hydride signals due to [(triphos)IrH_3{$AuP(i\text{-}Pr)_3$}$_2]^{2+}$, **B6**. As can be seen there, decoupling at the frequency of the P^{tr} atoms reduces the apparent doublet to triplets (actually a tripling of the AA′A″XX′X″ spin system pattern) to one triplet due to the $P(i\text{-}Pr)_3$ couplings (see Figure 3b), and decoupling at the frequency of the P^{Au} atoms leaves a spectrum similar to that of IrH_3(triphos) (see Figure 3c). Lowering the temperature to −80 °C results mainly in line broadening. Thus, this compound also remains fluxional in solution at this temperature. The ^1H NMR spectra of the other compounds can be related to that or **B6** by appropriate nuclear substitutions.

The IR spectra of complexes of this type in the region 1500–2400 cm^{-1} are best discussed considering the data on Figure 2a. As can be seen there, there is some residual absorption in the region corresponding to terminal Ir–H bonds as well as a broad absorption due to the Ir–H–Au bonds.

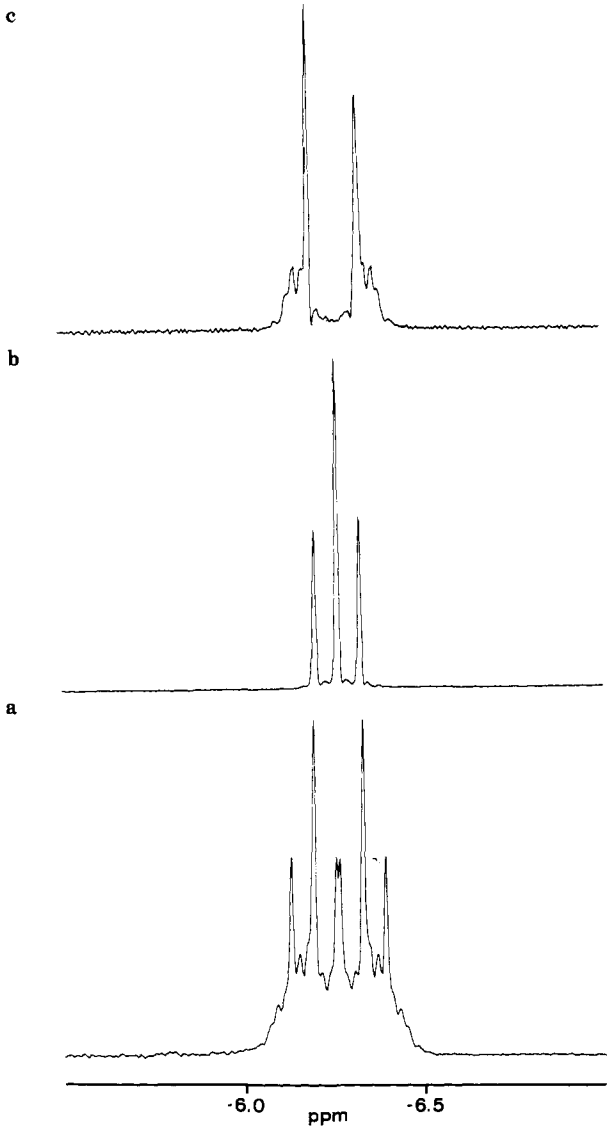

Figure 3. (a) 250 MHz ^1H NMR spectrum of $[(triphos)IrH_3\{Au(P(i\text{-}Pr)_3)\}_2](CF_3SO_3)_2$, **[B6]**$(CF_3SO_3)_2$; (b) 250 MHz $^1H\{^{31}P\}$ NMR spectrum of **[B6]**$(CF_3SO_3)_2$, decoupled at the ^{31}P resonance of P^{Ir}; (c) 250 MHz $^1H\{^{31}P\}$ NMR spectrum of **[B6]**$(CF_3SO_3)_2$, decoupled at the ^{31}P resonance of P^{Au}.

For complexes of type **B**, the proposed structures are analogous to that observed for $[(dppm)_2Ru(\mu\text{-}H)_2\{Au(PPh_3)\}_2]$ (V) (dppm = $Ph_2PCH_2PPh_2$).[21]

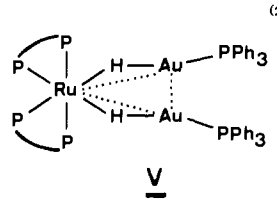

V

It is noteworthy here that in these complexes the two $Ru(\mu\text{-}H)Au$ units are mutually placed in such a way as to produce an Au–Au distance of 2.933 Å which can be taken as indicative of a significant direct interaction, as the Au–Au distance in metallic gold is 2.8782 Å.[22] By analogy, one can postulate that compounds of type B can be assigned the static structure shown below.

It is interesting to note that in V $J(P^{Au},\mu\text{-}H)$ is 75 Hz, while that found for the type **B** complexes is ca. 26 Hz. As for complexes

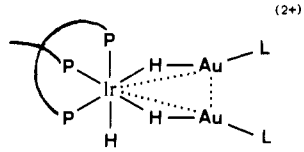

Type B

of type **A**, small couplings would be expected inasmuch as the gold phosphine units are highly mobile over three equivalent hydride positions.

An alternative structure will be proposed after the discussion of compounds of type **C**.

Complexes $[(tripod)MH_2\{Au(L)\}_3]^{2+}$, Type C. Addition of 3 molar equiv of $[Au(THF)(L)]^+$ to $MH_3(tripod)$ in CH_2Cl_2/THF does *not* give the expected complexes of the type $[(tripod)MH_3\{Au(L)\}_3]^{3+}$: only the corresponding compounds of type **B** and "free" $[Au(THF)(L)]^+$ are present in solution. However, in many cases addition of protic solvents, particularly methanol, to those solutions results in liberation of one proton with concomitant coordination of a third gold cation to the rhodium or iridium-forming compounds of type **C** (eq 3).

$$MH_3(tripod) + 3[Au(THF)(L)]^+ \xrightarrow[THF]{CH_2Cl_2} B +$$
$$[Au(THF)(L)]^+ \xrightarrow{MeOH} \underset{\text{type C}}{[(tripod)MH_2\{Au(L)\}_3]^{2+}} + \text{"}H^+\text{"} \quad (3)$$

M = Rh and Ir; tripod = triphos and triars;
L = tertiary phosphine or arsine

As found for complexes of the other types, the most basic structural information is provided by their NMR spectra. These are conveniently discussed using the static structure shown below for compound $[(triphos)IrH_2\{Au(PPh_3)\}_3]^{2+}$, **C4**.

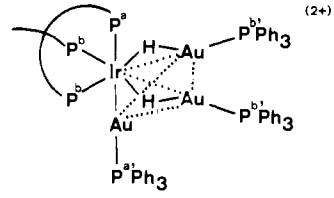

C4

The ^{31}P and ^1H NMR spectra are strongly temperature dependent, and therefore the low-temperature spectra will be discussed first.

At temperatures below −40 °C the ^{31}P NMR spectrum of **C4** shows three sets of resonances centered at −0.6, +6.5, and +50.2 ppm of relative intensities 2:1:3, which can be assigned to P^b, P^a, and $P^{a'} + P^{b'}$, respectively (see Table II and Figure 4a). This spectrum implies that at −40 °C, on the NMR time scale, $P^{a'}$ and $P^{b'}$ are dynamically equivalent. Thus this spectrum can be interpreted as arising from a "static" $IrH_2(triphos)$ framework, VI,

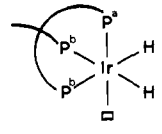

VI

with the Au_3 triangle rotating around the triangle defined by the two hydride ligands and the "vacant" coordination position. Thus the resonances due to $P^{a'} + P^{b'}$ (+50.2 ppm) would appear as a doublet of triplets because of their coupling to magnetically inequivalent P^a and two P^b atoms, while the signal assigned to P^b (−0.6 ppm) can be interpreted as an overlapping doublet of quartets. Finally, the multiplet assigned to P^a (+6.5 ppm) can be interpreted resulting from the overlap of a triplet of quartets.

The ^{31}P NMR low-temperature spectra of the other compounds can be assigned on the same basis taking into account the changes in NMR active nuclei. These assignments are confirmed by

(21) See ref in footnote 5.
(22) Pearson, W. B. *Lattice Spacings and Structures of Metals and Alloys*, 123; Pergamon Press: London, 1958.

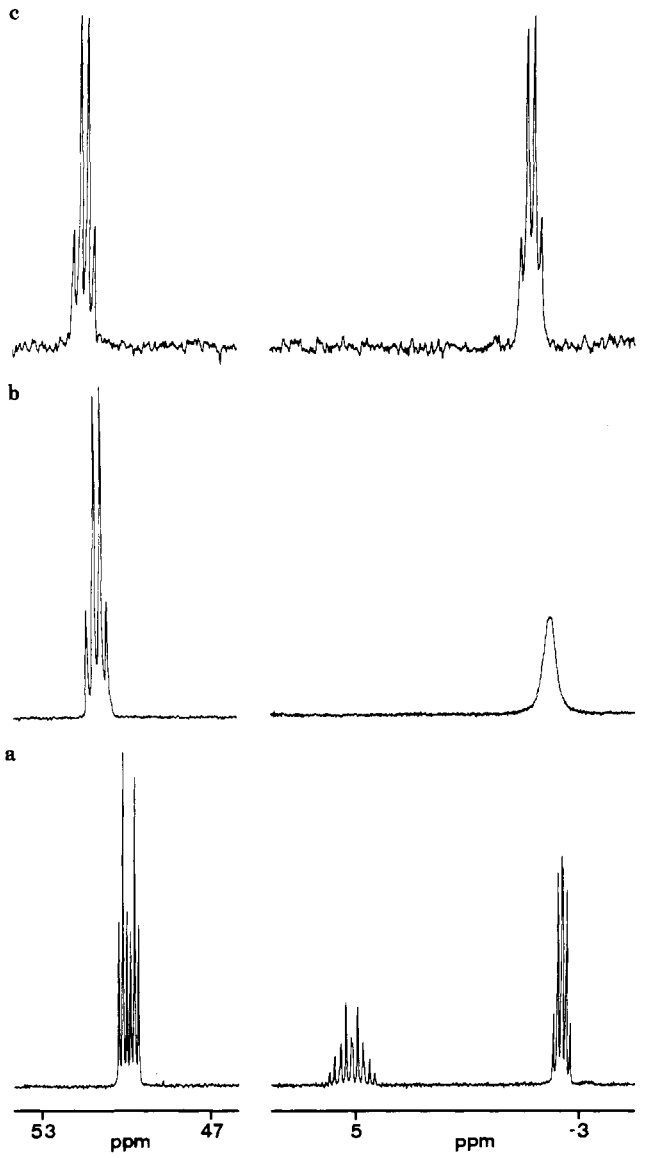

Figure 4. 101 MHz $^{31}P\{^1H\}$ NMR spectra of $[(triphos)IrH_2\{Au(PPh_3)\}_3](CF_3SO_3)_2$, [C4]$(CF_3SO_3)_2$: (a) recorded at −40 °C in CD_2Cl_2; (b) recorded at +25 °C in $CDCl_2CDCl_2$; (c) recorded at +80 °C in $CDCl_2CDCl_2$.

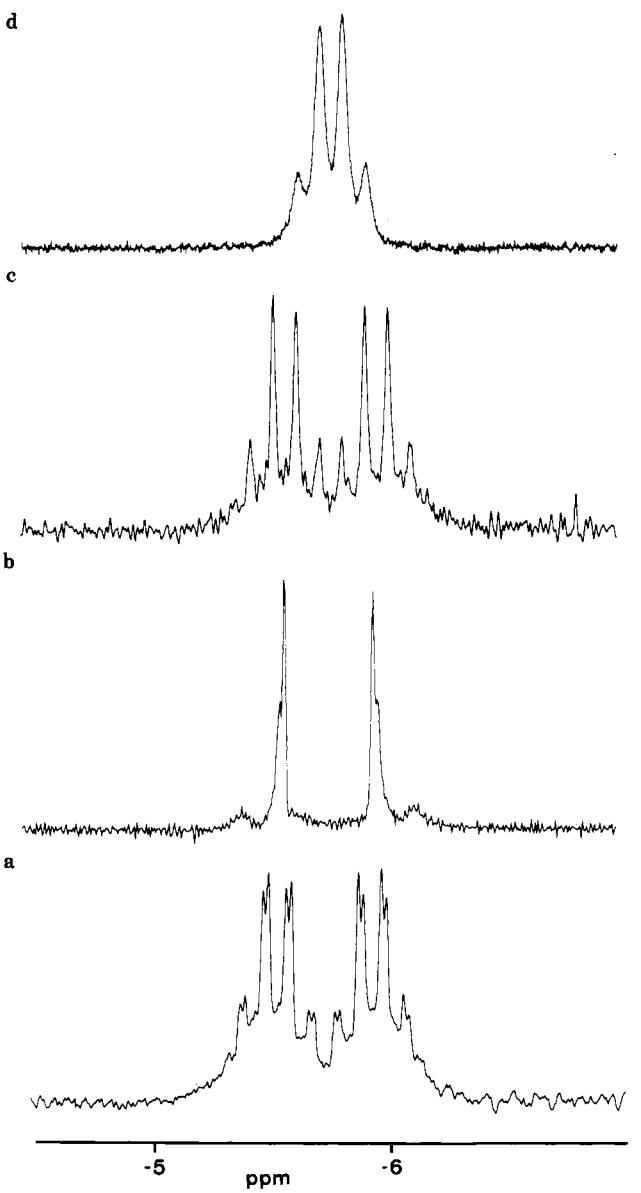

Figure 5. 250 MHz ^1H NMR spectra of $[(triphos)IrH_2\{Au(PPh_3)\}_3](CF_3SO_3)_2$, [C4]$(CF_3SO_3)_2$: (a) ^{31}P coupled spectrum; (b) ^{31}P decoupled at the ($P^{a'}$ + $P^{b'}$) resonance; (c) ^{31}P decoupled at the P^a resonance; (d) ^{31}P decoupled at the P^b resonance.

comparing the spectra of **C4** with those of $[(triphos)IrH_2\{Au(AsPh_3)\}_3]^{2+}$, **C8**, and $[(triars)IrH_2\{Au(PPh_3)\}_3]^{2+}$, **C10**. Thus, (1) replacement of PPh_3 in **C4** by $AsPh_3$, **C8**, results in a spectrum in which the resonances due to P^b appear as a doublet and those of P^a appear as a triplet, while (2) replacement of triphos in **C4** by triars, **C10**, gives a spectrum in which $P^{a'}$ + $P^{b'}$ give rise to a singlet. When the spectrum of **C4** is recorded at −100 °C, the dynamic behavior of $P^{a'}$ and $P^{b'}$ nuclei appears to be sufficiently slowed down to show nonequivalence between $P^{a'}$ and $P^{b'}$.

The low-temperature (−40 °C) ^1H NMR spectrum of **C4**, in the hydride region, appears as a doublet of quartets (see Figure 5) the individual resonances showing an additional small coupling. This spectrum is consistent with the spin system AA′MM′M″XYY′ where the A nuclei are the H ligands, M the P^{Au} donors, and X and Y the P^{tr} atoms. The largest coupling (that between the quartets) arises from the P^b atoms (Y) in trans position to hydrogen. The quartet arises from coupling with the three dynamically equivalent ($P^{a'}$ + $P^{b'}$) atoms bonded to gold (M,M′,M″). The small residual coupling results from interaction with the P^a atoms (X) and P^b atoms (Y′) in cis position to H. Selective ^{31}P decoupling experiments confirm these assignments. Thus, when the $P^{a'}$ and $P^{b'}$ nuclei are decoupled, the resulting spectrum (see Figure 5b) is consistent with an AA′XYY′ spin system analogous to that found in $IrH_2Cl(triphos)$.[11] On the other hand, when the P^a nucleus is decoupled, the small coupling disappears, and the resulting multiplet has the appearance of a doulet of quartets. On the basis of the AA′MM′M″XYY′ spin system one would expect to observe a small residual coupling due to the P^b atom (Y′) in cis position to hydrogen. However, while this coupling is not obvious, the signal-to-noise ratio is such that it cannot be excluded. Finally, irradiation at P^b leaves a broad quartet due to the coupling to the three $P^{a'}$ + $P^{b'}$ atoms. The coupling due to the P^a atom is not resolved but is indicated by the increased line width of the signals (8 Hz at half height).

The low-temperature ^1H NMR spectra, in the hydride region, of the other compounds can be interpreted on the same basis, and the data are presented in Table II.

As mentioned earlier, the ^{31}P and ^1H NMR spectra are strongly temperature-dependent. The ^{31}P NMR spectrum of **C4** is shown in Figure 4. As can be seen there, at room temperature (Figure 4b) the signals due to P^a and P^b appear as a single broad resonance, while those due to $P^{a'}$ and $P^{b'}$ give rise to a quartet. At +80 °c (Figure 4c) the signals due to P^a and P^b sharpen to a quartet while the multiplicity of $P^{a'}$ and $P^{b'}$ signals remain unchanged. These data can be interpreted by assuming that also the fragment "IrH_2(triphos)" has become fluxional, and, therefore, P^a and P^b

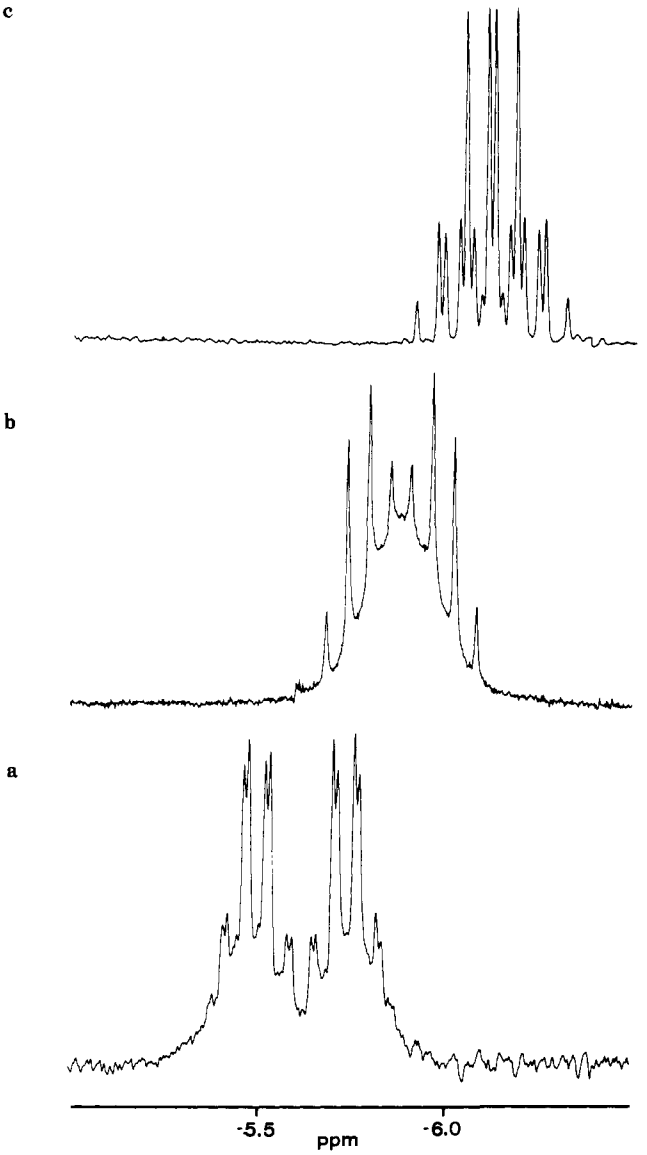

Figure 6. 250 MHz ^1H NMR spectra of $[(triphos)IrH_2\{Au(PPh_3)\}_3](CF_3SO_3)_2$, [C4]$(CF_3SO_3)_2$: (a) recorded at −40 °C in CD_2Cl_2; (b) recorded at +25 °C in $CDCl_2CDCl_2$; (c) recorded at +80 °C in $CDCl_2CDCl_2$.

become dynamically equivalent at this temperature. The room temperature spectrum then represents the intermediate dynamic range.

As can be seen from Figure 4b the broad signal due to P^{tr} is shifted to higher field relative to the position expected for a coalescence situation, i.e., between the signals observed for the static case. However, this difference must be attributed to the use of different solvents to cover the temperature range. Thus, the spectrum at −40 °C was recorded in CD_2Cl_2, while the spectra at room temperature and at +80 °C were recorded in $CDCl_2CDCl_2$.

The temperature dependence of the ^1H NMR spectrum of compound **C4** is shown in Figure 6. The spectrum at +80 °C (Figure 6c) is consistent with the model proposed on the basis of the ^{31}P NMR data at the same temperature, i.e., dynamic equivalence of the three P^{tr} and P^{Au} atoms, giving a quartet of quartets in a first-order description of the spectrum. Again, as in the ^{31}P NMR spectrum, the room temperature multiplet represents the intermediate dynamic range.

Although integration of the hydride signals relative to the CH_3 group of the organic ligand in each compound gave a ratio of 2(±0.1):3 and the solution, after reaction had occurred, was acidic, further confirmation of the presence of only two coordinated hydrides was obtained by recording the ^{103}Rh(DEPT) spectrum

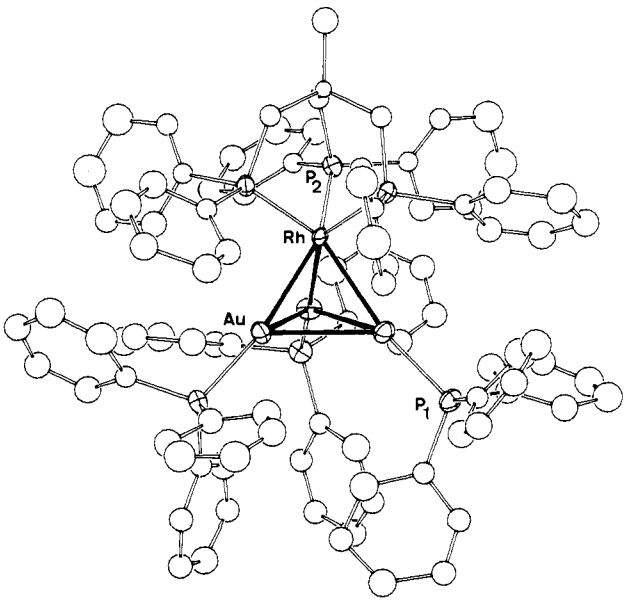

Figure 7. An ORTEP view of the cation **C1**.

Table III. Relevant Bond Lengths (Å) and Angles (deg) for Cation **C1**

Rh-Au	2.695 (2)	P2-C211	1.77 (2)
Au-Au′[a]	2.887 (1)	P2-C221	1.92 (2)
Au-P1	2.260 (5)	P2-C231	1.83 (2)
Rh-P2	2.313 (5)	C211-C212	1.57 (2)
P1-C[b]	1.80 (2)	C212-C231	1.59 (5)
Rh-Au-P1	167.9 (1)	Rh-P2-C211	110.1 (6)
Au-Rh-P2	87.7 (1)	Rh-P2-C221	113.7 (6)
Au-Rh-P2	144.0 (1)	Rh-P2-C231	123.8 (7)
Au′-Au-P1	131.0 (1)	P2-C211-C212	120.0 (1.4)
Au-Rh-Au′	64.78 (6)	C211-C212-C213	108.4 (1.1)
Rh-Au-Au′	57.61 (3)	C211-C212-C211′	110.5 (1.0)
P2-Rh-P2′	90.5 (2)		

[a] Primed atoms are related to those unprimed by one of the symmetry operations: $\bar{y}, x-y, z$; $\bar{x}+y, \bar{x}, z$. [b] Average value; the esd on the mean is estimated from the formula $\sigma(\bar{x}) = [\sum(x_1 - \bar{x})^2/n(n-1)]^{1/2}$, where $\bar{x}$ is the mean value and n is the number of observations.

of $[(triars)RhH_2\{Au(AsPh_3)\}_3]^{2+}$, **C3**.[23] This showed the expected triplet structure and the parameters are given in Table II. It is noteworthy that $^1J(^{103}Rh,^1H)$ is only 13 Hz, while it is 23 Hz in RhH_3(triars). Decreases in M-H coupling constants on hydrido-bridge formation, i.e., M-H-M′, have been observed for a variety of complex types.[12,23]

The IR spectra of compounds of type **c** do not show bands unambiguously assignable to terminal M-H vibrations. Broad regions of absorption are however, present e.g., by comparing the spectra of the parent MH_3(tripod) complexes with those of the corresponding species of type **C**. In the case of compound **C4** these occur at ca. 1625 and 1800 cm^{-1} (see Figure 2b).

X-ray Structure Analysis of $[(triphos)Rh(\mu\text{-}H)_2\{Au(PPh_3)\}_3](CF_3SO_3)_2$, [C1]$(CF_3SO_3)_2$. The crystal structure consists of discrete $[(triphos)Ru(\mu\text{-}H)_x\{Au(PPh_3)\}_3]$ cations and disordered $CF_3SO_3^-$ anions. The molecular structure of **C1** is presented in Figure 7. Selected bond distances and angles are given in Table III.

The molecular structure of **C1** can best be described as a metallotetrahedrane made up of a triangle of gold atoms capped by the rhodium triphos fragment. Attached to each gold is one PPh_3 ligand. The cation lies on a crystallographic 3-fold axis which goes through CH_3-C bond of triphos, the rhodium atom, and the center of the Au_3 triangular face. Thus, all three Rh-Au and Au-Au separations are equal at 2.695 (2) and 2.888 (1) Å, respectively, as are the Au-P and Rh-P distances (2.260 (5) and

(23) The ^{103}Rh(DEPT) NMR spectra were recorded by Dr. Clemens Anklin at Spectrospin AG in Fällanden, Switzerland.

Table IV. Comparison of Selected Structural Parameters for $[(triphos)Rh(\mu\text{-}H)_2\{Au(PPh_3)\}_3]^{2+}$ (**C1**), $[(PMe_2Ph)_3Re(\mu\text{-}H)_3\{Au(PPh_3)\}_3]^{+}$ (VII), and $[(PPh_3)_2(CO)Rh(\mu\text{-}H)\{Au(PPh_3)\}_3]^{+}$ (VIII)

		C1	VII	VIII
M-Au	(Å)	2.695 (2)	2.723 (1)	2.722
				2.664
				2.640
Au-Au	(Å)	2.888 (1)	2.931 (2)	2.914
				2.889
				2.814
M-P	(Å)	2.313 (5)	2.391 (5)	2.361
				2.353
Au-P	(Å)	2.260 (5)	2.267 (5)	2.29 (1)
				2.27 (1)
				2.23 (1)
M-Au-P	(deg)	167.9 (1)	167.8 (1)	172.2 (3)
				170.8 (3)
				165.2 (3)

2.313 (5) Å, respectively). The hydride ligands could not be located.

The microanalytical data obtained on solid samples of complexes of type **C**, including $[\mathbf{C1}](CF_3SO_3)_2$, are consistent with the solution data which clearly shows the presence of two hydride ligands and two triflate anions. Although the disorder of the latter in crystalline $[\mathbf{C1}](CF_3SO_3)_2$ prevented a reliable determination of their occupancy factor, i.e., their total number, the best fit with the experimental data is obtained assuming the presence of two $CF_3SO_3^-$ anions per cluster unit. However, *there is no evidence of disorder in the cluster unit* which might indicate that the C_3 axis is not a molecular symmetry axis. This rules out the presence of structures containing either (1) two static $Rh(\mu\text{-}H)Au$ and one unbridged RhAu units or (2) two static $Rh(\mu_3\text{-}H)Au_2$ and one unbridged $RhAu_2$ moieties with consequent changes in metal–metal bonding parameters. Thus, given the known mobility of hydrogen on cluster faces,[2c] the most likely interpretation of the observed struture is that of an $RhAu_3$ tetrahedron with two hydrogen atoms undergoing rapid site exchange among the three equivalent $RhAu_2$ triangular faces. On the other hand, on the basis of the crystal data one cannot rule out a static structure in which the two hydride ligands are located on the C_3 axis, e.g., one inside and the other outside the tetrahedron. Further studies, e.g., neutron scattering, will be required to make a reliable structural assignment.

Two structurally related heterometallic gold tetrahedranes have been reported recently: $[(PMe_2Ph)_3Re(\mu\text{-}H)_3\{Au(PPh_3)\}_3]^{+}$ (VII)[24] and $[(PPh_3)_2(CO)Rh(\mu\text{-}H)\{Au(PPh_3)\}_3]^{+}$ (VIII).[25]

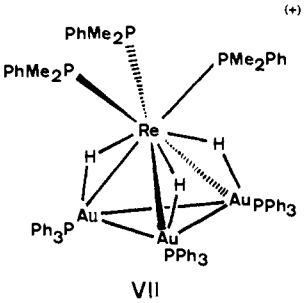

VII

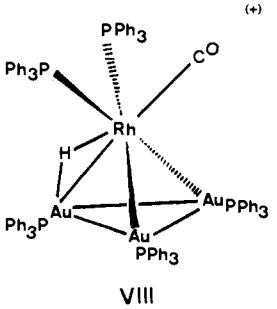

VIII

Selected structural parameters for **C1**, VII, and VIII are given in Table IV. The three structures have several common features: (1) the average Au–Au bond distance in each cluster is close to that found in gold metal (2.8782 Å);[22] (2) the observed Au–P distances are equal within the standard deviations; (3) the M–Au–P angles of **C1** and VII are identical with and close to those found in VIII (av 169°).

However, a closer comparison of the three structures reveals two significant differences: (1) the MAu_3 tetrahedron is symmetrical in **C1** and VII but distored in VIII; (2) the triangle defined by the P atoms coordinated to rhodium in **C1** are almost eclipsed as seen by the dihedral angle P(1)–Au(1)–Rh–P(2) which is 15°, while the corresponding angles in VII and VIII are 2° and 78°, respectively; (3) the Re–Au distances are longer than the Rh–Au distances as would be expected from the differences in the bonding radii of Re and Rh.[26]

It is noteworthy that clusters **C1**, VII, and VIII are also isoelectronic; each cluster contains 54 electrons. While this is six electrons less than what is predicted for tetrahedral metal carbonyl clusters, the gold heterometallics should not be considered electron deficient. In fact, they are electron precise, inasmuch as each gold only contributes one cluster valence molecular orbital—the hy(s-z) hybrid orbital (see above).[27,28]

Finally, it should be pointed out that the solid-state data and the dynamic behavior observed in solution are consistent as, in the crystal, the rotation of the Au_3 moiety relative to the rhodium triphos unit is frozen to give an eclipsed conformation. A possible explanation for the structural irregularity of the MAu_3 tetrahedron in VIII may be the presence of different ligands on rhodium.

The structural considerations developed for the type **C** clusters can be extended also to the corresponding type **B** compounds, given the isolobality of "H^+" and "AuL^+".[29] Thus the complexes of type **C** are isolobal with those of type **B**, and, therefore, the latter can be formulated as hydrido–digold–monoiridium(rhodium) tetrahedral clusters.

The Relative Stabilities of Compounds of the Type A, B, and C. As can be seen in Table I, a wide range of complexes of the above types have been prepared. The relative stabilities of the iridium complexes will be discussed first as a more extensive set of complexes has been investigated. The following trends are apparent.

(1) The presence of coordinated alkyl phosphines on gold prevents the formation of complexes of type C. The formation of type **C** complexes can be rationalized on the general assumption that an increase in the number of coordinated gold cations to the parent trihydride withdraws increasing amounts of electron density from the resulting heterometallic complex up to the point where, when two gold cations are bound to the trihydride complex, the third hydride ligand is insufficiently basic to form an M–H–Au bond. The driving force for the formation of type **C** complexes is then, as expected, provided by the protonation of the basic solvent.

One plausible model that can be postulated for the transformation of complexes of type **B** into the corresponding species of type **C** is based on the relative "acidity" of the hydride ligand in a complex of type **B** undergoing the reaction shown in eq 4.

$$L'_nIr\text{-}H + S + AuL^+ \rightleftharpoons L'_nIr\text{-}AuL + SH^+ \quad (S = \text{solvent}) \qquad (4)$$

This is equivalent to the isolobal substitution of "H^+" by "AuL^+".[29] Thus, the ease of deprotonation of the type **B** complex should depend on the acidity of the Ir–H terminal hydride which, in turn, will be influenced by changes in Lewis acid character of the $[AuL]^+$ species already bound to M. Then the weaker Lewis acidity of $[Au(PEt_3)]^+$ relative to $[Au(PPh_3)]^+$ would reduce the tendency for the formation of complexes of type **C** in the former case.

(2) The presence of the very bulky P(o-Tol)$_3$ (Tolman's cone angle = 194°) also prevents the formation of a complex of type C. It is not surprising that electronic effects mentioned above are insufficient to overcome the effect of steric bulk of phosphine

(24) Sutherland, B. R.; Folting, K.; Streib, W. E.; Ho, D. M.; Huffman, J. C.; Caulton, K. G. *J. Am. Chem. Soc.* **1987**, *109*, 3489.
(25) Boyle, P. D.; Johnson, B. J.; Buehler, A.; Pignolet, L. H. *Inorg. Chem.* **1986**, *25*, 7.
(26) See reference in footnote 9.
(27) Lauher, J. W. *J. Am. Chem. Soc.* **1978**, *100*, 5305.
(28) The authors are indebted to a referee for the suggestion that "it is better to consider [this type of cluster as] a single rhodium complex with five of its ligands undergoing the same type of association found in dihydrogen complexes".
(29) Lavigne, G.; Papageorgiou, F.; Bonnet, J.-J. *Inorg. Chem.* **1984**, *23*, 609 and references quoted therein. See also references in footnotes 7d, 14, and 22.

ligands on gold, as found in the case of the $P(o\text{-Tol})_3$ complexes.

(*3*) *The coordination of an arsine ligand on gold destabilizes type* ***B*** **complexes**. While it is possible to prepare solutions containing complexes such as $[(triphos)IrH_3Au(AsPh_3)]^+$ **A8**, attempts to obtain the corresponding complexes of type **B** by mixing solutions of the Ir hydride and of the Au cation in a 1:2 ratio one often give, in addition to the expected compound, significant amounts of the corresponding complexes of type **A** and type **C**. Their amount increases with time indicating the disproportion reaction: $2\mathbf{B8} + S \rightarrow \mathbf{A8} + \mathbf{C8} + SH^+$. This reaction is complete within 12 h in solution.

The replacement of the phosphine donor on gold by an arsine, because of the weaker donor capacity of the latter (at parity of R groups),[30] makes $[Au(AsR_3)]^+$ a stronger Lewis acid than the corresponding $[Au(PR_3)]^+$ and, therefore, favors the loss of a proton.

The tendency prevents the isolation of complexes of type **B** as attempts to crystallize them lead to the formation of complexes of type **A** and **C**.

However, steric bulk of the arsine ligands, e.g., $As(i\text{-Pr})_3$, on gold prevents the formation of type **C** complexes and therefore the disproportion reaction is no longer possible, so that the complex $[(triphos)IrH_3\{AuAs(i\text{-Pr})_3\}_2]^{2+}$, **B9**, is stable in solution.

(*4*) *Replacement of triphos by triars also destabilizes the complexes of type* ***B*** and, as in the case above, does not allow the isolation of these reaction intermediates. The replacement of triphos by triars is expected to decrease the electron density at iridium because of the lower electron donor capacity of arsenic relative to phosphorus at parity of R groups.[30] This, in turn will reduce the partial negative charge on the hydride ligand in the arsine complex relative to the phosphine complex and therefore lead to more facile deprotonation.

(5) Although the rhodium complexes of type **A**, **B**, and **C** have not been extensively investigated, present indications are that *rhodium and iridium show the same trends, the only noticeable difference being that the rhodium complexes decompose more easily with deposition of metallic gold.* This decomposition appears to be photochemically induced; the iridium complexes are also photosensitive but to a lesser extent than the corresponding rhodium compounds.

The proclivity of transition-metal hydrides to reduce gold(I) with formation of metal–metal bonds, much in the same manner as $NaBH_4$, has been noted elsewhere.[25] In this regard, eq 3 can be viewed as a reduction of the Rh/Ir center, with the formation of a metal–metal bond (type **C** complexes) and concomitant oxidation of the hydride ligand to a proton. Since type **C** complexes only form in a relatively polar solvent (MeOH), the reaction appears to be thermodynamically disfavored except when a suitable acceptor for the leaving proton is present. This notion is in accord with recent results reported by Sutherland et al.[24] in which $[(PMe_2Ph)_3Re(\mu\text{-}H)_3\{Au(PPh_3)\}_3]^+[OR]^-$ (VII) (R = 2,4,6-tris-^{t}Bu-phenoxide) readily eliminates ROH in benzene to yield $(PMe_2Ph)_3Re(\mu\text{-}H)_2\{Au(PPh_3)\}_3$ (IX), while the BF_4^- salt is stable.

Our results, while in agreement with transition-metal hydrides functioning as sources of electrons in cluster formation, also suggest that hydride species can play the role of templates, bridging several equivalents of gold(I) phosphine in close proximity (type **A** and **B** complexes) before actual electron transfer occurs (type **C** complexes). The initial bonding is presumably a result of metal hydride donation into the empty hy(s-z) hybrid orbital of $[Au(PPh_3)]^+$.[14] Thus it is perhaps not surprising that an intermediate hydride species is required before metal–metal bonds are formed between $[Au(PPh_3)]^+$ and $[Ir(dppe)_2]^+$, a coordinatively unsaturated complex.[31]

Experimental Section

Physical Measurements and Reagents. The ^1H NMR spectra were recorded at 250.13 MHz on a Bruker WM-250 instrument, while ^{31}P NMR spectra were recorded either at 36.43 MHz on a Bruker HX-90 or at 101.26 MHz on a Bruker WM-250 instrument. The ^1H NMR spectra are referenced to external Me_4Si, while the ^{31}P NMR spectra are referenced to external H_3PO_4 with a positive sign indicating a chemical shift downfield of the reference. The ^{103}Rh NMR spectra were measured on a Bruker AC-250 spectrometer at 7.91 MHz by using conventional INEPT[32] or DEPT[33] sequences. Chemical shifts for ^{103}Rh are reported relative to 3.16 MHz with the field set so that TMS resonates at exactly 100 MHz, giving chemical shifts in ppm to high frequency of the reference. CD_2Cl_2 was dried over P_2O_5 and vacuum transferred prior to use. Infrared spectra were recorded on a Perkin-Elmer 1430 spectrophotometer as CsI pellets.

All manipulations of the rhodium compounds were carried out under a nitrogen atmosphere using standard Schlenk techniques. Unless otherwise stated the iridium complexes were prepared in air. The solvents were used as purchased from FLUKA AG for the iridium chemistry but were dried and distilled under nitrogen prior to use for the rhodium compounds.

The complexes $AuCl(PPh_3)$, $AuCl(PEt_3)$, $AuCl(P\{i\text{-Pr}\}_3)$, $AuCl(P\{o\text{-Tol}\}_3)$, $AuCl(AsPh_3)$, and $AuCl(As\{i\text{-Pr}\}_3)$ were prepared as described in the literature.[34] The chlorides $RhCl_3$(triars) and $IrCl_3$(triars) and the hydrides RhH_3(triphos),[10] RhH_3(triars), IrH_3(triphos),[11] and IrH_3(triars) were prepared as described below.

$RhCl_3$(triars). It was prepared by mixing 5 g (19 mmol) of $RhCl_3 \cdot 3H_2O$ and 14.4 g (19 mmol) of triars in 100 mL of ethanol. The mixture was heated to reflux for 15 h. The yellow precipitate was then filtered off and washed with ethanol and ether: yield 17.5 g (95%).

$IrCl_3$(triars). It was obtained as a yellow precipitate by the above procedure, using 5 g (12 mmol) of $IrCl_3 \cdot xH_2O$ (iridium content 46%) and 9.08 g (12 mmol) of triars: yield 11.2 g (98%).

RhH_3(triphos). A yellow suspension of 5 g (6 mmol) of $RhCl_3$(triphos)[35] in 50 mL of ethanol was cooled in a ice bath, and 1.36 g (36 mmol) of solid $NaBH_4$ were then added. The mixture was stirred for 15 min at 0 °C, removed from the ice bath, and allowed to warm up to room temperature during another 15 min. The slightly brownish suspension was heated under reflux for about 20 min to ensure that all $NaBH_4$ had reacted. The deep brown-reaction mixture was then cooled in an ice bath, and the fine brownish precipitate was filtered off and washed twice with cold ethanol and dried in vacuum. The crude product (3.73 g) was redissolved in 20 mL of CH_2Cl_2, and 50 mL of ethanol were rapidly added. Precipitation was completed by removing the CH_2Cl_2 under vacuum, leaving small off-white needles: yield 2.85 g (65%).

RhH_3(triars). It was prepared as an off-white powder by the above procedure, using 4.83 g (5 mmol) of $RhCl_3$(triars) and 1.13 g (30 mmol) of $NaBH_4$: yield 2.59 g (60%).

IrH_3(triphos). This compound was prepared under a nitrogen atmosphere. Solid $LiAlH_4$ (10-g package as purchased from FLUKA AG) in 200 mL of ether was heated under reflux for 2 h. The remaining gray precipitate was allowed to settle, and the solution was filtered off. This clear colorless solution was added to a suspension of 5 g (5.4 mmol) of $IrCl_3$(triphos)[35] in 100 mL of THF until almost all solid had dissolved (volumes between 30 and 50 mL were usually required, depending upon the quality of the $LiAlH_4$), and a pale yellow cloudy solution was obtained. Upon warming a white precipitate began to form. after 30 min the mixture was cooled to room temperature, the nitrogen stream was stopped, but stirring was maintained for another 3 h under laboratory atmosphere. Hydrolysis was then completed with a few drops of water followed by addition of 200 mL of 15% aqueous NaOH. The resulting slurry was extracted with three 200-mL portions of CH_2Cl_2. The organic layers were collected, dried over $MgSO_4$, and evaporated to dryness. Crystallization of the crude product from CH_2Cl_2/hexane yielded 3.54 g (80%) of white needles.

IrH_3(triars). It was prepared by the procedure described above, using 528 mg (0.5 mmol) of $IrCl_3$(triars) in 10 mL of THF and 20 mL of the saturated solution of $LiAlH_4$ in ether. Since dissolution of the solid was not observed, the reaction mixture was heated overnight. Hydrolysis with 50 mL of 15% aqueous NaOH and extraction with three 50-mL portions of CH_2Cl_2 yielded 240 mg (50%) of an off-white powder.

Preparation of the Rhodium/Iridium–Gold Complexes. These were prepared by one of two general methods, depending on the reagent ($Tl[PF_6]$ or $AgCF_3SO_3$) used for the abstraction of the chloride from AuCl(L).

(30) Ahrland, S.; Berg, T.; Bläuenstein, P. *Acta Chem. Scand. A* **1978**, *32*, 933 and references quoted therein.

(31) Casalnouvo, A. L.; Laska, T.; Nilsson, P. V.; Olofson, J.; Pignolet, L. H. *Inorg. Chem.* **1985**, *24*, 233.

(32) Morris, G. A.; Freeman, R. *J. Am. Chem. Soc.* **1979**, *101*, 760.

(33) Bendall, M. R.; Doddrell, D. M..; Pegg, D. T.; Hull, W. E. *J. Magn. Reson.* **1981**, *44*, 238.

(34) McAuliffe, C. A.; Parish, R. V. D.; Randall, P. D. *J. Chem. Soc., Dalton Trans.* **1979**, 1730.

(35) Siegl, W. O.; Lapporte, S. J.; Collman, J. P. *Inorg. Chem.* **1971**, *10*, 2158.

Method A. A solution of $Tl[PF_6]$ in THF was added to a CH_2Cl_2 solution containing the hydride MH_3(tripod) and the gold–phosphine/arsine complex. The cloudly solution was stirred for 15 min and was then evaporated to dryness. The residue was suspended to CH_2Cl_2 and filtered through Celite. In most cases the crude product was recrystallized by dissolving it in one solvent, and then adding a second solvent until a turbidity appeared. A few drops of the first solvent were added to obtain a clear solution (if this did not occur the mixture was filtered again) which was then stored at ca. −20 °C. The solvents used or any departure from this procedure are given below. Yields ranged between 70% and 90%.

Method B. A solution of $AgCF_3SO_3$ in THF was added to another solution of the corresponding gold–phosphine/arsine complex in THF. The mixture was stirred for 15 min. The white AgCl precipitate formed was coagulated by warming up the suspension to about 60 °C. It was then filtered through Celite, and the colorless solution was added to a solution of the hydride MH_3(tripod) in CH_2Cl_2 (usually, at this stage more AgCl precipitated from the reaction mixture). The solvents were removed under reduced pressure, the residue was suspended in CH_2Cl_2 and filtered again through Celite, and the solution was taken to dryness under reduced pressure. Unless mentioned otherwise, the products were recrystallized by the general procedure described in method A. Yields ranged between 60% and 90%.

$[RhAuH_3(PPh_3)(triphos)][PF_6]$, [A1][$PF_6$]. It was prepared by method A using 22 mg (0.044 mmol) of $AuCl(PPh_3)$ and 32 mg (0.044 mmol) of RhH_3(triphos) in 5 mL of CH_2Cl_2 and 15 mg (0.044 mmol) of $Tl[PF_6]$ in 5 mL of THF. Crystallization from CH_2Cl_2/ether yielded a white precipitate which was washed with ether: yield 49 mg (85%). Anal. Calcd for $C_{59}H_{57}AuF_6P_5Rh$: C, 53.08; H, 4.31. Found: C, 52.22; H, 4.44.

$[RhAu_2H_3(PPh_3)_2(triphos)][PF_6]_2$, [B1][$PF_6$]$_2$. It was prepared by method A using 37 mg (0.075 mmol) of $AuCl(PPh_3)$ and 27 mg (0.037 mmol) of RhH_3(triphos) in 5 mL of CH_2Cl_2 and 26 mg (0.075 mmol) of $Tl[PF_6]$ in 5 mL of THF. The crude product was dissolved in 3 mL of CH_2Cl_2 and placed in a Schlenk tube. A second tube which contained 5 mL of ether was connected through a side arm. Storage overnight at room temperature yielded a yellow-white solid which was collected and washed with ether: yield 63 mg (87%). Anal. Calcd for $C_{77}H_{72}Au_2F_{12}P_7Rh$: C, 47.69; H, 3.75. Found: C, 47.48; H, 3.70.

$[RhAu_3H_2(PPh_3)_3(triphos)][PF_6]_2$, [C1][$PF_6$]$_2$. It was prepared by method A using 104 mg (0.210 mmol) of $AuCl(PPh_3)$ and 51 mg (0.070 mmol) of RhH_3(triphos) in 10 mL of CH_2Cl_2 and 73 mg (0.210 mmol) of $Tl[PF_6]$ in 5 mL of THF. Crystallization from CH_2Cl_2/MeOH yielded yellow microcrystals which were washed with MeOH and ether: Yield 133 mg (79%). Anal. Calcd for $C_{95}H_{86}Au_3F_{12}P_8Rh$: C, 47.59; H, 3.62. Found: C, 47.19; H, 3.58.

$[RhAu_3H_2(AsPh_3)_3(triphos)][PF_6]_2$, [C2][$PF_6$]$_2$. It was prepared by method A using 113 mg (0.210 mmol) of $AuCl(AsPh_3)$ and 51 mg (0.070 mmol) of RhH_3(triphos) in 10 mL of CH_2Cl_2 and 73 mg (0.210 mmol) of $Tl[PF_6]$ in 5 mL of THF. Crystallization from CH_2Cl_2/MeOH yielded yellow microcrystals which were washed with MeOH and ether: yield 129 mg (73%). Anal. Calcd for $C_{95}H_{86}As_3Au_3F_{12}P_5Rh$: C, 45.12; H, 3.43. Found: C, 45.49; H, 3.69.

$[RhAu_3H_2(AsPh_3)_3(triars)][PF_6]_2$, [C3][$PF_6$]$_2$. It was prepared by method A using 210 mg (0.38 mmol) of $AuCl(AsPh_3)$ and 110 mg (0.13 mmol) of RhH_3(triars) in 10 mL of CH_2Cl_2 and 130 mg (0.38 mmol) of $Tl[PF_6]$ in 5 mL of THF. Crystallization from CH_2Cl_2/MeOH yielded yellow microcrystals which were washed with MeOH and ether: yield 340 mg (62%). Anal. Calcd for $C_{95}H_{86}As_6Au_3F_{12}P_2Rh$: C, 42.88; H, 3.26. Found: C, 42.93; H, 3.17.

$[IrAuH_3(PPh_3)(triphos)](CF_3SO_3)$, [A4]($CF_3SO_3$). It was prepared by method **B** using 50 mg (0.10 mmol) of $AuCl(PPh_3)$ and 26 mg (0.10 mmol) of $AgCF_3SO_3$ in 6 mL of THF and 82 mg (0.10 mmol) of IrH_3(triphos) in 5 mL of CH_2Cl_2. Recrystallization from CH_2Cl_2/hexane yielded a white powder. Elemental analyses were not satisfactory due to decomposition in solution. Therefore the [BPh_4] salt, **$[IrAuH_3(PPh_3)(triphos)][BPh_4]$, [A4][$BPh_4$]**, was prepared. The crude reaction mixture obtained as described above was redissolved in 10 mL of MeOH, and 170 mg (0.5 mmol) of Na[BPh_4] in 5 mL of MeOH were added with stirring. The white solid was collected and washed with MeOH and ether: yield 113 mg (71%). Anal. Calcd for $C_{83}H_{77}AuBIrP_4$: C, 62.37; H, 4.86. Found: C, 61.67; H, 5.02.

$[IrAu_2H_3(PPh_3)_2(triphos)](CF_3SO_3)_2$, [B4]($CF_3SO_3$)$_2$. It was prepared by method **B** using 99 mg (0.20 mmol) of $AuCl(PPh_3)$ and 51 mg (0.20 mmol) of $AgCF_3SO_3$ in 8 mL of THF and 82 mg (0.10 mmol) of IrH_3(triphos) in 5 mL of CH_2Cl_2. Dissolution of the crude product in CH_2Cl_2, precooled to −80 °C, followed by rapid precipitation with hexane yielded a white powder which was washed with ether: yield 173 mg (85%). Anal. Calcd for $C_{79}H_{72}Au_2F_6Au_2IrO_6P_5S_2$: C, 46.59; H, 3.56. Found: C, 46.11; H, 3.63.

$[IrAu_3H_2(PPh_3)_3(triphos)](CF_3SO_3)_2$, [C4]($CF_3SO_3$)2. It was prepared by method **B** using 148 (0.30 mmol) of $AuCl(PPh_3)$ and 77 mg (0.30 mmol) of $AgCF_3SO_3$ in 10 mL of THF and 82 mg (0.10 mmol) of IrH_3(triphos) in 5 mL of CH_2Cl_2. Recrystallization from CH_2Cl_2/MeOH yielded yellow cubes which were washed with MeOH and ether: yield 230 mg (92%). Anal. Calcd for $C_{97}H_{86}Au_3F_6IrO_6P_6S_2$: C, 46.70; H, 3.47. Found: C, 46.48; H, 3.66.

$[IrAuH_3(PEt_3)(triphos)](CF_3SO_3)$, [A5]($CF_3SO_3$). It was prepared by method **B** using 35 mg (0.10 mmol) of $AuCl(PEt_3)$ and 26 mg (0.10 mmol) of $AgCF_3SO_3$ in 6 mL of THF and 82 mg (0.10 mmol) of IrH_3(triphos) in 5 mL of CH_2Cl_2. Recrystallization from THF/hexane yielded a white powder which was washed with hexane and ether: yield 82 mg (64%). Anal. Calcd for $C_{48}H_{57}AuF_3IrO_3P_4S$: C, 44.90; H, 4.47. Found: C, 44.79; H, 4.58.

$[IrAu_2H_3(PEt_3)_2(triphos)](CF_3SO_3)_2$, [B5]($CF_3SO_3$)$_2$. It was prepared by method **B** using 70 mg (0.20 mmol) of $AuCl(PEt_3)$ and 51 mg (0.20 mmol) of $AgCF_3SO_3$ in 8 mL of THF and 82 mg (0.10 mmol) of IrH_3(triphos) in 5 mL of CH_2Cl_2. Recrystallization from THF/ether yielded a white powder which was washed with ether: yield 107 mg (61%). Anal. Calcd for $C_{55}H_{72}Au_2F_6IrO_6P_5S_2$: C, 37.79; H, 4.15. Found: C, 35.68; H, 4.37.

$[IrAuH_3(P\{i\text{-}Pr\}_3)(triphos)](CF_3SO_3)$, [A6]($CF_3SO_3$). It was prepared by method B using 39 mg (0.10 mmol) of $AuCl(P\{i\text{-}Pr\}_3)$ and 26 mg (0.10 mmol) of $AgCF_3SO_3$ in 6 mL of THF and 82 mg (0.10 mmol) or IrH_3(triphos) in 5 mL of CH_2Cl_2. Recrystallization from THF/hexane yielded a white powder which was washed with hexane and ether: yield 107 mg (81%). Anal. Calcd for $C_{51}H_{63}AuF_3IrO_3P_4S$: C, 46.19; H, 4.79. Found: C, 45.84; H, 4.75.

$[IrAu_2H_3(P\{i\text{-}Pr\}_3)_2(triphos)](CF_3SO_3)_2$, [B6]($CF_3SO_3$)$_2$. It was prepared by method **B** using 79 mg (0.20 mmol) of $AuCl(P\{i\text{-}Pr\}_3)$ and 51 mg (0.20 mmol) of $AgCF_3SO_3$ in 8 mL of THF and 82 mg (0.10 mmol) of IrH_3(triphos) in 5 mL of CH_2Cl_2. Recrystallization from THF/ether yielded a white powder which was washed with ether: yield 125 mg (68%). Anal. Calcd for $C_{61}H_{84}Au_2F_6IrO_6P_5S_2$: C, 39.98; H, 4.62. Found: C, 39.94; H, 4.80.

$[IrAuH_3(P\{o\text{-}Tol\}_3)(triphos)](CF_3SO_3)$, [A7]($CF_3SO_3$). It was prepared by method **B** using 54 mg (0.10 mmol) of $AuCl(P\{o\text{-}Tol\}_3)$ and 26 mg (0.10 mmol) of $AgCF_3SO_3$ in 6 mL of THF and 82 mg (0.10 mmol) of IrH_3(triphos) in 5 mL of CH_2Cl_2. Recrystallization from CH_2Cl_2/hexane yielded a white powder which was washed with hexane and ether: yield 134 mg (91%). Anal. Calcd for $C_{63}H_{63}AuF_3IrO_3P_4S$: C, 51.46; H, 4.32. Found: C, 50.62; H, 4.48.

$[IrAu_2H_3(P\{o\text{-}Tol\}_3)_2(triphos)](CF_3SO_3)_2$, [B7]($CF_3SO_3$)$_2$. It was prepared by method B using 108 mg (0.20 mmol) of $AuCl(P\{o\text{-}Tol\}_3)$ and 51 mg (0.20 mmol) of $AgCF_3SO_3$ in 8 mL of THF and 82 mg (0.10 mmol) of IrH_3(triphos) in 5 mL of CH_2Cl_2. Recrystallization from THF/hexane yielded a white powder which was washed with hexane and ether: yield 148 mg (72%). Anal. Calcd for $C_{85}H_{84}Au_2F_6IrO_6P_5S$: C, 48.14;, H, 3.99. Found: C, 48.43; H, 4.27.

$[IrAuH_3(AsPh_3)(triphos)][PF_6]$, [A8][$PF_6$]. It was prepared by method A using 82 mg (0.10 mmol) of IrH_3(triphos) and 54 mg (0.10 mmol) of $AuCl(AsPh_3)$ in 8 mL of CH_2Cl_2 and 35 mg (0.10 mmol) of $Tl[PF_6]$ in 5 mL of THF. The mixture was stirred for 15 min and was then filtered through Celite, and the solvents were removed under reduced pressure. The crude product was dissolved in 3 mL of warm $CHCl_3$. This solution was filtered again and allowed to cool down to room temperature. It was then stored at ca. −20 °C overnight. The colorless crystals were then filtered off and washed with hexane and ether: yield 125 mg (85%). Anal. Calcd for $C_{59}H_{57}AsAuF_6IrP_4$: C, 48.27; H, 3.91. Found: C, 47.71; H, 3.87.

$[IrAu_2H_2(AsPh_3)_2(triphos)][PF_6]_2$, [B8][$PF_6$]$_2$. Solutions of this compound were prepared by method A using 108 mg (0.20 mmol) of $AuCl(AsPh_3)$ and 82 mg (0.10 mmol) of IrH_3(triphos) in 5 mL of CH_2Cl_2 and 35 mg (0.10 mmol) of $Tl[PF_6]$ in 5 mL of THF. However, depending on the reaction time, these solutions contained different amounts of the disproportion products **A8** and **C8** as mentioned in the Discussion Section. Solutions of [**B8**](CF_3SO_3)$_2$ prepared by method **B** decomposed even faster. Thus, recrystallization was impossible, and elemental analysis is not available.

$[IrAu_3H_2(AsPh_3)_3(triphos)](CF_3SO_3)_2$, [C8]($CF_3SO_3$)$_2$. It was prepared by method B using 162 mg (0.30 mmol) of $AuCl(AsPh_3)$ and 77 mg (0.30 mmol) of $AgCF_3SO_3$ in 10 mL of THF and 82 mg (0.10 mmol) of IrH_3(triphos) in 5 mL of CH_2Cl_2. Recrystallization from CH_2Cl_2/MeOH (very little CH_2Cl_2 should be used here) yielded yellow cubes which were washed with MeOH and ether: yield 187 mg (71%). Anal. Calcd for $C_{97}H_{86}As_3Au_3F_6IrO_6P_3S_2$: C, 44.36; H, 3.30. Found: C, 44.12; H, 3.42.

$[IrAuH_3(As\{i\text{-}Pr\}_3)(triphos)][PF_6]$, [A9][$PF_6$]. It was prepared by method A using 82 mg (0.10 mmol) of IrH_3(triphos) and 44 mg (0.10 mmol) of $AuCl(As\{i\text{-}Pr\}_3)$ in 8 mL of CH_2Cl_2 and 35 mg (0.10 mmol)

Table V. Experimental Data[a] for the X-ray Diffraction Study of [C1]$(CF_3SO_3)_2$

formula	$C_{97}H_{86}Au_3F_6O_6P_6RhS_2$
mol wt	2405.510
cryst dimens, mm	0.3 × 0.3 × 0.2
cryst syst	trigonal
space group	$R3c$
a, Å	20.343 (3)
c, Å	44.937 (7)
Z	6
V, Å^3	16104.9
ρ(calcd), g cm^{-3}	1.486
μ, cm^{-1}	65.61
radiation	Mo K$\bar{\alpha}$ (graphite monochromated; λ = 0.71069 Å)
measd reflcns	$\pm h,+k,+l$
θ range, deg	$2.3 \le \theta \le 24.5$
scan type	$\omega/2\theta$
max scan speed, deg min^{-1}	20.3
scan width, deg	1.1 + 0.35 tan θ
max counting time, s	65
prescan rejectn lim	0.5 (2σ)
prescan acceptnce lim	0.03 (33σ)
bkgd time	0.5 × scan time
horiz receiving aperture, mm	1.9 + tan θ
vert receiving aperture, mm	4.0
no. of data collected	9405
no. of indep data	2205
no. of obsd data ($I_{obsd} \ge 2.0\sigma(I_{obsd})$)	1833
agreement on av[b]	0.02
no. of variables refined	158
R[c]	0.049
R_w[d]	0.080

[a] Data collected at room temperature. [b] $R_{av} = \sum|\bar{F}_o^2 - (F_o)_i^2|/\sum\bar{F}_o^2$. [c] $R = \sum(||F_o| - 1/k|F_c||)/\sum|F_o|$. [d] $R_w = [\sum w(|F_o| - 1/k|F_c|)^2/\sum wF_o^2]^{1/2}$. $w = [\sigma^2(F_o)]^{-1}$ and $\sigma(F_o) = [\sigma^2(F_o^2) + f^2(F_o^2)]^{1/2}/2F_o$ with f = 0.040.

of Tl[PF_6] in 3 mL of THF. Recrystallization from $CHCl_3$/hexane yielded a white powder which was washed with hexane and ether: yield 95 mg (70%). Anal. Calcd for $C_{50}H_{60}AsAuF_6IrP_4$: C, 44.06; H, 4.44. Found: C, 44.05; H, 4.82.

[$IrAu_2H_3$(As{*i*-Pr}$_3$)$_2$(triphos)][PF_6]$_2$, [**B9**][PF_6]$_2$. It was prepared by method A using 82 mg (0.10 mmol) of IrH_3(triphos) and 88 mg (0.20 mmol) of AuCl(As{*i*-Pr}$_3$) in 8 mL of CH_2Cl_2 and 70 mg (0.20 mmol) of Tl[PF_6] in 3 mL of THF. Recrystallization from THF/ether yielded a white powder which was washed with hexane and ether: yield 134 mg (70%). Anal. Calcd for $C_{59}H_{81}As_2Au_2F_{12}IrP_5$: C, 37.12; H, 4.28. Found: C, 36.99; H, 4.47.

[$IrAu_3H_2$(PPh$_3$)$_3$(triars)](CF_3SO_3)$_2$, [**C10**](CF_3SO_3)$_2$. It was prepared by method B using 74 mg (0.15 mmol) of AuCl(PPh_3) and 39 mg (0.15 mmol) of $AgCF_3SO_3$ in 10 mL of THF and 48 mg (0.05 mmol) of IrH_3(triars) in 5 mL of CH_2Cl_2. Recrystallization from CH_2Cl_2/EtOH yielded a yellow powder which was washed with EtOH and ether: yield 105 mg (80%). Anal. Calcd for $C_{97}H_{86}As_3Au_3F_6IrO_6P_3S_2$: C, 44.36; H, 3.30. Found: C, 43.99; H, 3.24.

Preparation of [$RhAu_3H_2$(AsPh$_3$)$_3$(triars)](CF_3SO_3)$_2$, [C3](CF_3SO_3)$_2$. Compound [**C3**](CF_3SO_3)$_2$ was prepared according to the procedure used for the preparation of the corresponding iridium analogue [**C4**](CF_3SO_3)$_2$ with the difference that oxygen was excluded. Crystals suitable for X-ray diffraction studies were obtained from dichloromethane/1,2-dichloroethane (1/1) solutions by layering with hexane.

Determination and Refinement of the Structure of [(triphos)RhH_2(AuPPh$_3$)$_3$](CF_3SO_3)$_2$, [C1](CF_3SO_3)$_2$. X-ray Measurements. Crystals of [**C1**](CF_3SO_3)$_2$ were obtained as described above. A small colorless prismatic crystal was mounted at a random orientation on a glass fiber. Space group and cell constants were determined on a Nonius CAD4 diffractometer that was subsequently used for the data collection. The symmetry of the crystal is trigonal, and the systematic absences are consistent with the space groups $R3c$ and $R\bar{3}c$. The noncentrosymmetric $R3c$ group was chosen and confirmed by the determined geometry and the successful refinement.

Cell constants were obtained by a least-squares fit of 25 high angle reflections ($10.0° \le \theta \ge 15.9°$) by using the CAD4 centering routines[36] and are listed along with other crystallographic data in Table V. Three reflections were chosen as standards to check the decay of the crystal and the stability of the experimental conditions and measured every hour; the crystal orientation was checked by measuring three standards every 300 reflections.

Data were collected at variable scan speed to ensure constant statistical precision of the measured intensities. A total of 9405 reflections ($\pm h,+k,+l$) were measured and corrected for Lorentz and polarization factors and for decay (correction factors in the range 0.99–1.10). An absorption correction was then calculated by using the Ψ scans of three reflections at high χ angle ($\chi \ge 85.0°$). The corrected data were averaged to give a set of 2205 independent reflections of which 1833 were considered as observed having $F_o^2 \ge 2.0\sigma(F_o^2)$, while $F_o^2 = 0.0$ was given to those reflections having negative net intensities.

The structure was solved by Patterson and Fourier methods and refined by full-matrix least squares, minimizing $(\sum w(|F_o| - (1/k)|F_c|)^2)$. No extinction correction was applied.

The scattering factors used, corrected for the anomalous dispersion,[37] were taken from tabulated values.[36]

Anisotropic temperature factors were used for the Rh, Au, P, and S atoms, while isotropic parameters were used for the others. The contribution of the hydrogen atoms held fixed in their calculated positions (C–H = 0.95 Å, B_{iso} = 8.0 Å^2) was also taken into account. The $CF_3SO_3^-$ counterion was found to be highly disordered: the Fourier difference maps showed residual peaks the highest of about 1.5–2.0 e$^-$/Å^3 near the S, O, and F atoms. The disorder was modeled assuming six positions for the O and F and two for the S atoms. This model refined successfully, leading to an acceptable geometry even though with high thermal parameters. Moreover, different occupancy factors for the anions were also tried; the best results were obtained for an occupancy factor corresponding to a 1:2 cation/anion ratio. All calculations were carried out with the Nonius SDP package. The handedness of the crystal was tested by refining the two possible sets of coordinates and comparing the R_w factors.[38] The positional parameters corresponding to the lowest R_w are listed in the Supplementary material (Table S1).

Acknowledgment. P. Janser carried out the work during the tenure of a research fellowship of the Swiss National Science Foundation, while L. F. Rhodes received support from the Forschungskommission der ETH Zürich. A Albinati acknowledges the support of the Italian National Research Council. We are greatly indebted to Prof. P. S. Pregosin for much valuable advice and to Dr. C. Anklin for measurement of the ^{103}Rh NMR.

Registry No. [**A1**][PF_6], 118474-12-7; [**A4**][BPh_4], 118474-14-9; [**A5**](CF_3SO_3), 118474-16-1; [**A6**](CF_3SO_3), 118474-18-3; [**A7**](CF_3SO_3), 118474-20-7; [**A8**][PF_6], 118474-22-9; [**A91**][PF_6], 118474-24-1; [**B1**][PF_6]$_2$, 118473-86-2; [**B4**](CF_3SO_3)$_2$, 118473-88-4; [**B5**](CF_3SO_3)$_2$, 118473-90-8; [**B6**](CF_3SO_3)$_2$, 118473-92-0; [**B7**](CF_3SO_3)$_2$, 118473-94-2; [**B8**][PF_6]$_2$, 118473-96-4; [**B9**][PF_6]$_2$, 118473-98-6; [**C1**][PF_6]$_2$, 118494-01-2; [**C1**](CF_3SO_3)$_2$, 118474-00-3; [**C2**][PF_6]$_2$, 118474-02-5; [**C3**][PF_6]$_2$, 118494-02-3; [**C3**](CF_3SO_3)$_2$, 118474-04-7; [**C4**](CF_3SO_3)$_2$, 118474-06-9; [**C8**](CF_3SO_3)$_2$, 118474-08-1; [**C10**](CF_3SO_3)$_2$, 118474-10-5; AuCl(PPh_3), 14243-64-2; AuCl(PEt_3), 15529-90-5; AlCl(P{*i*-Pr}$_3$), 33659-45-9; AuCl(P{*o*-Tol}$_3$), 28978-10-1; AuCl($AsPh_3$), 25749-29-5; AuCl(As{*i*-Pr}$_3$), 118473-80-6; $RhCl_3$(triars), 118473-81-7; $IrCl_3$(triars), 118473-82-8; RhH_3(triphos), 100333-94-6; RhH_3(triars), 118473-83-9; IrH_3(triphos), 104453-08-9; IrH_3(triars), 118473-84-0; $RhCl_3$(triphos), 62792-06-7; $IrCl_3$(triphos), 104453-05-6; Au, 7440-57-5; Rh, 7440-16-6; Ir, 7439-88-5.

Supplementary Material Available: Table S1, positional parameters; Table S2, thermal factors; Table S4, extended bond lengths and angles, and Figure S1, numbering scheme for the cation **C3** (14 pages); listing of observed and calculated structure factors (13 pages). Ordering information is given on any current masthead page.

(36) Enraf-Nonius Structure Determination Package (SDP); Enraf-Nonius: Delft, Holland, 1980.
(37) *International Tables for X-ray-Crystallography*; Kynoch: Birmingham, England, 1974; Vol. IV.
(38) Hamilton, W. C. *Acta Crystallogr.* **1965**, *13*, 502.